PHYSICAL REVIEW E VOLUME 62, NUMBER 4 OCTOBER 2000

Coupling between tilt and polar orders in liquid crystal phases formed from achiral bent shaped molecules

Pierre Tolédano,[1,2] Odair G. Martins,[1] and Antonio M. Figueiredo Neto[1]
[1]*Instituto de Física, Universidade de São Paulo, Caixa Postal 66318, 05315-970, São Paulo, SP, Brazil*
[2]*Groupe Structure des Materiaux Sous Conditions Extrêmes, SNBL/ESRF, 38043 Grenoble Cedex, France*

(Received 29 November 1999; revised manuscript received 9 June 2000)

A phenomenological description is given of the mesophases which may arise below a liquid formed from achiral molecules possessing a transverse dipole, as the result of a coupling between their tilt and polar orders. Six stable mesophases are found. Two of them have a cholesteric biaxial structure. The others display antiferroelectric or ferrielectric, incommensurately modulated, structures with in-plane or out-of-plane spontaneous polarization. The in-plane polarized structures become unstable under application of a longitudinal electric field. Other field-induced effects are discussed.

PACS number(s): 61.30.Cz, 77.84.Nh

I. INTRODUCTION

After having been the subject of discussions in preliminary studies [1,2] the possibility of obtaining chiral liquid crystal phases by the spontaneous organization of achiral molecules was demonstrated experimentally [3,4]. Antiferroelectric smectic domains formed from molecules with bent cores that are achiral were obtained, with two types of tilted configurations displaying alternate or identical handedness from layer to layer [4]. Subsequently the synthesis of a variety of liquid crystal compounds with ‘‘banana’’ shaped molecules was reported [5], showing different phases with homogeneous [3–6] or helical [7] structures.

Within the smectic layers the bent geometry of the molecules allows a polar order perpendicular to the director $\hat{n}$, defined as the average direction of the long axes which lie along the line joining the two ends of the bent molecules. The molecules may also have a tilted organization with respect to the layer normal, with a wave vector $\hat{k}$. Therefore, the molecular configurations result from the coupling of two symmetry breaking instabilities, which are the polar orientational order and the molecular tilt. Depending on the nature of the parent paraelectric phase these two instabilities possess either different or identical symmetries.

(1) Starting from a parent smectic-*A* (Sm*A*) phase of achiral point group $D_{\infty h}$, in which the bent molecules rotate freely around their long axes, the polar and tilt orders are associated with distinct two-component order parameters which are biquadratically coupled. Such a situation was considered by Roy *et al.* [8], who showed that five different smectic configurations of the achiral molecules within the smectic layers could be stabilized. Two of these configurations possess a spontaneous longitudinal polarization, compatible with the $\hat{n}\rightarrow-\hat{n}$ symmetry, and give rise to remarkable field effects [8].

(2) Assuming a parent liquid state, as reported experimentally up to now [3–7], the polar and tilt orders have the same symmetry, corresponding to four-component order parameters related by a bilinear coupling. Taking into account only the polar order, Lorman and Mettout [9] described theoretically the resulting ordered phases, which have the structure of a vector wave with transverse linear, circular, or elliptic polarizations. In their study these authors neglected the influence of the tilt order, considering that the condensation of the tilt wave necessarily induces the polarization wave, and vice versa [9].

The aim of the present paper is to extend the work of Ref. [9], showing that in contrast to the preceding presupposition the coupling of the tilt and polar waves, in a liquid formed from achiral bent shaped molecules (or any achiral molecules permitting a transverse polar order), allows stabilization of additional stable phases, displaying remarkable effects. In particular we show that taking into account the coupling between the two instabilities leads to antiferroelectric and ferrielectric phases which possess a longitudinal component of the polarization, compatible with the $\hat{n}\rightarrow-\hat{n}$ symmetry. The paper is organized as follows. In Sec. II the homogeneous equilibrium molecular configurations which may form below the liquid are worked out. In Sec. III the corresponding macroscopic structures are described, considering the inhomogeneous couplings between the tilt and polar waves, as well as the homogeneous coupling which results in a smectic ordering. In Sec. IV the influence of an applied, longitudinal, or transverse electric field on the different mesophase structures is discussed. Finally (Sec. V), we summarize our results, and briefly discuss the available experimental data on ‘‘banana’’ shaped molecular systems.

II. EQUILIBRIUM MOLECULAR CONFIGURATIONS

We start from a liquid state formed from achiral polar molecules, and assume that as the medium is cooled a transition takes place to a phase resulting from the simultaneous condensation of a transverse axial vector wave (expressing the molecular tilt with respect to the $\hat{k}$ direction) and a polar vector wave. The axial vector wave of molecular tilt can be defined as

$$\vec{\xi}(z)=[\xi_x\cos(kz+\tilde{\varphi}_x)]\vec{\tilde{e}}_x+[\xi_y\cos(kz+\tilde{\varphi}_y)]\vec{\tilde{e}}_y, \quad (1)$$

where the coordinate z is taken along the $\hat{k}$ direction, and $|\hat{k}|=k$. ξ_x and ξ_y are the transverse wave amplitudes. $\tilde{\varphi}_x$ and

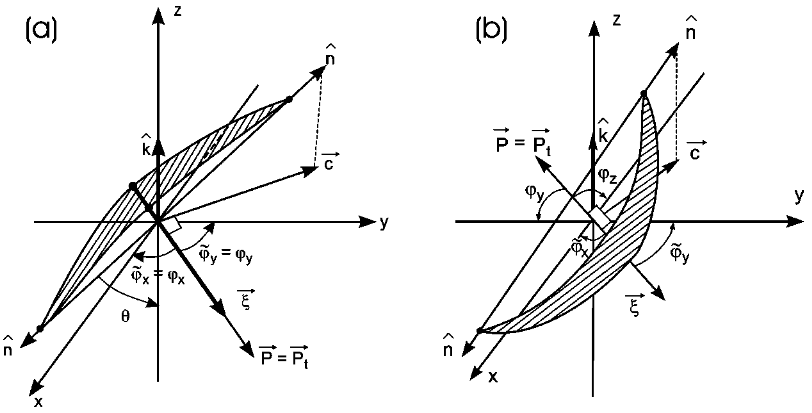

FIG. 1. Local molecular configuration associated with (a) in-phase and (b) opposed-phase tilt and polar waves.

$\tilde{\varphi}_y$ are the initial phases. $\tilde{\vec{e}}_x$ and $\tilde{\vec{e}}_y$ are axial unit vectors in the plane perpendicular to $\hat{k}$. The polar vector wave can be written in the general case as the sum of transverse and longitudinal components, $\vec{P}(z) = \vec{P}_t(z) + P_z\vec{e}_z$, $\vec{e}_z$ being the unit-vector along z, where the transverse component is defined in a similar way as $\vec{\xi}(z)$:

$$\vec{P}_t(z) = [P_x \cos(kz + \varphi_x)]\vec{e}_x + [P_y \cos(kz + \varphi_y)]\vec{e}_y. \quad (2)$$

P_x and P_y are the polar-wave amplitudes, and $\vec{e}_x$ and $\vec{e}_y$ the unit vectors in the direction perpendicular to $\hat{k}$.

Assuming the $\hat{k}$ direction to be determined, $\vec{\xi}(z)$ and $\vec{P}_t(z)$ transform as the same four-dimensional irreducible representation of the Euclidean symmetry group $O(3)\times R_3$, denoted $G_{\hat{k}}$, whose generating 4×4 matrices are given in the Appendix. Using the notation of Ref. [9], the four components of the corresponding irreducible order parameters can be written for $\vec{\xi}(z)$ as $\xi_1 = \xi_x e^{i\tilde{\varphi}_x} - i\xi_y e^{i\tilde{\varphi}_y}$, $\xi_2 = -\xi_x e^{-i\tilde{\varphi}_x} + i\xi_y e^{-i\tilde{\varphi}_y}$, $\xi_3 = \xi_1^*$, and $\xi_4 = \xi_2^*$. For $\vec{P}_t(z)$, one has $\eta_1 = P_x e^{i\varphi_x} - iP_y e^{i\varphi_y}$, $\eta_2 = P_x e^{-i\varphi_x} - iP_y e^{-i\varphi_y}$, $\eta_3 = \eta_1^*$, and $\eta_4 = \eta_2^*$. Using the transformation properties of the ξ_i and η_i $(i = 1-4)$ components by $G_{\hat{k}}$, one finds the following independent invariants:

$$\begin{aligned}
I_1 &= \xi_1\xi_1^* + \xi_2\xi_2^* = 2(\xi_x^2 + \xi_y^2),\\
I_2 &= \xi_1\xi_1^*\xi_2\xi_2^* = I_1^2 - 4\xi_x^2\xi_y^2 \sin^2(\tilde{\varphi}_x - \tilde{\varphi}_y),\\
I_1' &= \eta_1\eta_1^* + \eta_2\eta_2^* = 2(P_x^2 + P_y^2), \quad (3)\\
I_2' &= \eta_1\eta_1^*\eta_2\eta_2^* = I_1'^2 - 4P_x^2P_y^2 \sin^2(\varphi_x - \varphi_y),\\
I_3 &= \eta_1\xi_1^* + \eta_1^*\xi_1 - \eta_2\xi_2^* - \eta_2^*\xi_2\\
&= 4[P_x\xi_x \cos(\varphi_x - \tilde{\varphi}_x) + P_y\xi_y \cos(\varphi_y - \tilde{\varphi}_y)].
\end{aligned}$$

In addition, the coupling between the longitudinal component P_z and the transverse axial and polar vector waves is

$$\begin{aligned}
I_4 &= P_z[\eta_1\xi_1^* - \eta_1^*\xi_1 + \eta_2\xi_2^* - \eta_2^*\xi_2]\\
&= 4P_z[P_x\xi_x \sin(\varphi_x - \tilde{\varphi}_x) + P_y\xi_y \sin(\varphi_y - \tilde{\varphi}_y)]. \quad (4)
\end{aligned}$$

Therefore, one can write the homogeneous part of the free-energy density F_h describing transitions from the liquid state as a function of the amplitude components ξ_x, ξ_y, P_x, P_y, and P_z, and dephasings between the transverse axial and polar waves $\varphi_1 = \varphi_x - \tilde{\varphi}_x$ and $\varphi_2 = \varphi_y - \tilde{\varphi}_y$. Restricting ourselves to the fourth degree monomials in the amplitude components, one has

$$\begin{aligned}
&F_h(\xi_x, \xi_y, P_x, P_y, P_z, \varphi_1, \varphi_2)\\
&= \frac{\alpha_1}{2}(\xi_x^2 + \xi_y^2) + \frac{\beta_1}{4}(\xi_x^2 + \xi_y^2)^2 + \frac{\beta_2}{2}\xi_x^2\xi_y^2 \sin^2(\tilde{\varphi}_x - \tilde{\varphi}_y)\\
&+ \frac{a_1}{2}(P_x^2 + P_y^2) + \frac{b_1}{4}(P_x^2 + P_y^2)^2\\
&+ \frac{b_2}{2}P_x^2P_y^2 \sin^2(\varphi_x - \varphi_y)\\
&+ \delta_1[P_x\xi_x \cos\varphi_1 + P_y\xi_y \cos\varphi_2]\\
&+ \frac{\delta_2}{2}[(\xi_x^2 + \xi_y^2)(P_x^2 + P_y^2)] + \frac{\delta_3}{2}[P_x\xi_x \cos\varphi_1\\
&+ P_y\xi_y \cos\varphi_2]^2 + \mu P_z[P_x\xi_x \sin\varphi_1 + P_y\xi_y \sin\varphi_2]\\
&+ \frac{1}{2\chi_{33}^o}P_z^2, \quad (5)
\end{aligned}$$

where α_1, β_1, β_2, a_1, b_1, b_2, δ_1, δ_2, δ_3, μ, and χ_{33}^o are phenomenological coefficients, which are assumed to be constant except $\alpha_1 = \alpha_o(T - T_c)$ and $a_1 = a_o(T - T_c)$. The dephasings $(\tilde{\varphi}_x - \tilde{\varphi}_y)$ and $(\varphi_x - \varphi_y)$ are determined by the equilibrium conditions

$$\begin{aligned}
&\xi_x^2\xi_y^2 \sin(\tilde{\varphi}_x - \tilde{\varphi}_y)\cos(\tilde{\varphi}_x - \tilde{\varphi}_y) = 0 \quad \text{and}\\
&P_x^2P_y^2 \sin(\varphi_x - \varphi_y)\cos(\varphi_x - \varphi_y) = 0, \quad (6)
\end{aligned}$$

which for $\xi_x\xi_y \neq 0$ and $P_xP_y \neq 0$ yield the equilibrium values $\tilde{\varphi}_x - \tilde{\varphi}_y = \pi/2$ and $\varphi_x - \varphi_y = \pi/2$, the solutions $\tilde{\varphi}_x = \tilde{\varphi}_y$ and $\varphi_x = \varphi_y$ corresponding to unstable states.

Minimization of F_h with respect to P_z gives the equilibrium value

$$P_z^e = -\mu\chi_{33}^o[P_x\xi_x \sin\varphi_1 + P_y\xi_y \sin\varphi_2], \quad (7)$$

showing that for $\varphi_1 \neq (0,\pi)$ or (and) $\varphi_2 \neq (0,\pi)$, i.e., for tilt and polar transverse waves which are not in phase or in

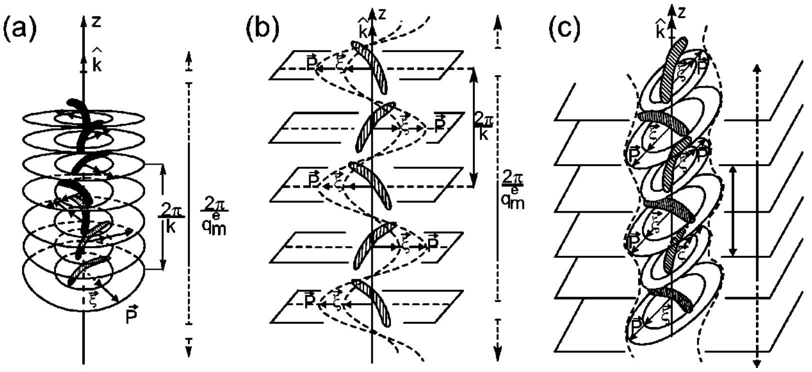

FIG. 2. Structure of the molecular configurations I, II, and III. (a) Circularly polarized configuration I, which gives rise to a biaxial cholesteric macroscopic structure of achiral symmetry D_∞. (b) Linearly polarized configuration II, which yields an antiferroelectric bilayer smectic structure for the mesophase. Each bilayer has the achiral symmetry mma. The macroscopic resulting symmetry is $mm2$. (c) Elliptically polarized configuration III. The chiral symmetry $P2_122$ of each bilayer is lowered to $P2$ under the effect of the long period modulation.

phase opposition, there exists a nonzero longitudinal component of the total polarization. Introducing P_z^e in Eq. (5) and minimizing F_h with respect to φ_1 and φ_2, one obtains the equations of state

$$P_x\xi_x\left[\sin\varphi_1\left(\delta_1+\frac{\delta_3}{4}I_3\right)-\mu\cos\varphi_1P_z^e\right]=0,$$

$$P_y\xi_y\left[\sin\varphi_2\left(\delta_1+\frac{\delta_3}{4}I_3\right)-\mu\cos\varphi_2P_z^e\right]=0, \tag{8}$$

where I_3 and P_z^e are given by Eqs. (3) and (7), respectively. Equations (8) and the minimization of F_h with respect to ξ_x, ξ_y, P_x, and P_y show that, in addition to the parent liquid state $(\xi_x=\xi_y=0, P_x=P_y=0)$, two classes of equilibrium molecular configurations can be distinguished.

(1) A first class is defined by the conditions $\sin\varphi_1=\sin\varphi_2=0$. The transverse tilt and polar waves are in phase $(\tilde{\varphi}_x=\varphi_x)$ or in phase opposition $(\tilde{\varphi}_x=\varphi_x+\pi, \tilde{\varphi}_y=\varphi_y+\pi)$, as represented in Figs. 1(a) and 1(b). As a consequence $P_z^e=0$, and the total polarization is transverse $(\vec{P}=\vec{P}_t)$, colinear to $\vec{\xi}$, and normal to the plane formed by $\hat{k}$ and $\hat{n}$ and the projection $\vec{c}$ of $\hat{n}$ in the (x,y) plane, i.e., the tilt occurs by a rotation of the molecules around the common in-plane direction determined by $\vec{\xi}$ and $\vec{P}$. A further minimization of F_h with respect to the components ξ_x, ξ_y, P_x, and P_y shows that the $\vec{\xi}$ and $\vec{P}$ vectors can be differently polarized in the plane perpendicular to $\hat{k}$.

(i) For $\xi_x=\xi_y=\xi_o\neq0$ and $P_x=P_y=P_o\neq0$, taking into account the conditions $\tilde{\varphi}_y=\tilde{\varphi}_x+(\pi/2)$ and $\varphi_y=\varphi_y+(\pi/2)$, one has $\vec{\xi}=\xi_o[\cos(kz+\tilde{\varphi}_x)\vec{e}_x+\sin(kz+\tilde{\varphi}_x)\vec{\varphi}_y]$ and $\vec{P}_t=P_o[\cos(kz+\varphi_x)\vec{e}_x+\sin(kz+\varphi_x)\vec{e}_y]$ defining *circularly polarized transverse waves*. Along z the $\vec{\xi}$ and $\vec{P}$ vectors describe concentric spirals with circular projections in the (x,y) plane and a periodicity $2\pi/k$ [Fig. 2(a)]. In terms of the ξ_i and η_i components such a configuration (denoted I hereafter) corresponds to the conditions $|\xi_1|\neq0, |\eta_1|\neq0$ and $|\xi_2|=0, |\eta_2|=0$, or equivalently to $|\xi_1|=0, |\eta_1|=0$ and $|\xi_2|\neq0, |\eta_2|\neq0$.

(ii) For $\xi_x=\xi_o\neq0, \xi_y=0$ and $P_x=P_o\neq0, P_y=0$ (or equivalently $\xi_y\neq0, \xi_x=0$ and $P_y\neq0, P_x=0$), Eqs. (1) and (2) have the simple forms $\vec{\xi}=\xi_o\cos kz\,\vec{e}_x$ and $\vec{P}_t=P_o\cos kz\,\vec{e}_x$, which describe *linearly polarized transverse waves*, varying periodically, with a periodicity $2\pi/k$ along z, as shown in Fig. 2(b). The ξ_i and η_i variables obey the conditions $|\xi_1|^2=|\xi_2|^2$ and $|\eta_1|^2=|\eta_2|^2$ for this configuration, denoted II hereafter.

(iii) For $\xi_x\neq\xi_y\neq0$ and $P_x\neq P_y\neq0$, Eqs. (1) and (2) and the conditions $\tilde{\varphi}_y=\tilde{\varphi}_x+(\pi/2)$ and $\varphi_y=\varphi_x+(\pi/2)$ correspond to *elliptically polarized transverse waves*, displaying a modulation of periodicity $2\pi/k$ along z for the long and short axes of the ellipses [Fig. 2(c)]. Here the equilibrium relationships $|\xi_1|\neq|\xi_2|\neq0$ and $|\eta_1|\neq|\eta_2|\neq0$ are fulfilled. This configuration will be denoted III.

(2) A second class of equilibrium configurations is stabilized for $\sin\varphi_1^e=\sin\varphi_2^e\neq0$, thus corresponding to arbitrary dephasings $(\tilde{\varphi}_x-\varphi_x)=(\tilde{\varphi}_y-\varphi_y)\neq(0,\pi)$. From Eqs. (8) one can deduce that φ_1^e and φ_2^e are temperature dependent, i.e., the relative orientation of the transverse tilt and polar waves $\vec{\xi}$ and $\vec{P}_t$ vary with temperature. On the other hand Eq. (7) shows that a nonzero component of the longitudinal polarization takes place: $P_z^e\neq0$. Hence the total polarization $\vec{P}$ has the orientation shown in Figs. 3(a) and 3(b): it is normal to $\hat{n}$ and fulfill the $\hat{n}\rightarrow-\hat{n}$ symmetry requirement. In other words, the tilt mechanism corresponds here to an inclination of the molecules with respect to the z axis, within the $(\vec{c},\vec{k})$ plane, where $\vec{k}$ here is a vector since the $\vec{k}\rightarrow-\vec{k}$ symmetry of the phase is broken. Minimizing F_h with respect to ξ_x, ξ_y, P_x, and P_y again yields three stable molecular configurations, denoted I′, II′, and III′, which correspond to transverse waves which are circularly, linearly, and elliptically polarized, as for configurations I, II, and III. Thus in the configurations I′ and III′, which are stabilized for $(\xi_x=\xi_y$ and $P_x=P_y)$ and $(\xi_x\neq\xi_y, P_x\neq P_y)$, respectively, the $\vec{\xi}$ and $\vec{P}$ vectors describe circular and elliptic dephased spirals, which are shifted with respect to one another along z, as shown in Figs. 4(a) and 4(c). The configuration II′ which corresponds to

$$\cos\varphi_1^e=-\frac{\delta_1(\delta_3+\mu^2\chi_{33}^o)^{-1}}{P_x\xi_x}$$

and $(\xi_x\neq0, \xi_y=0, P_x\neq0, P_y=0)$, coincides with a transverse wave linearly polarized, but showing a *canting* of the polarization $\vec{P}$ with respect to the z direction [Fig. 4(b)].

Table I summarizes the equilibrium properties of the six configurations enumerated here above. Configurations I, II, and III coincide with the ordered states described theoretically in Ref. [9]. Note that we have considered exclusively

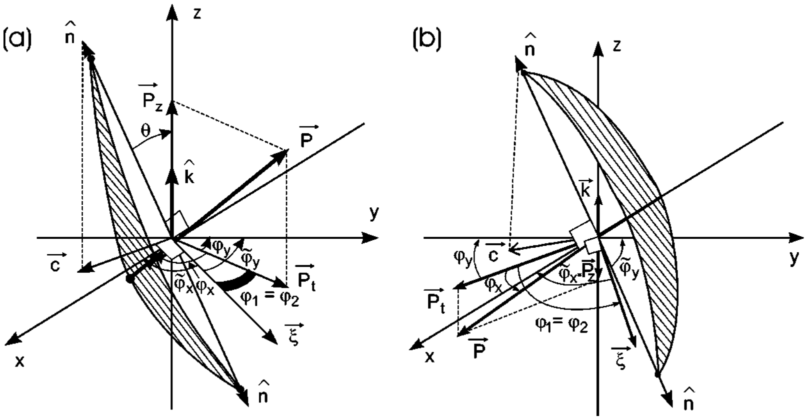

FIG. 3. Local molecular configuration associated with dephased tilt and polar transverse waves. (a) and (b) show configurations with opposed polarizations.

the configurations which result from a coupling between tilt and polar orders, assuming that the nonzero (ξ_x,ξ_y) and (P_x,P_y) components appear simultaneously at the same critical temperature T_c, as is usually observed in ferroelectric or antiferroelectric smectic phases. Indeed, the minimization of the free-energy F_h also leads to stable states in which the tilt and polar orders are uncoupled and may appear at distinct critical temperatures. Thus for $\varphi_1=\varphi_2=\pm\pi/2$, one finds two additional states, which have been also included in Table I: (i) State IV, corresponding to $\xi_x=\xi_y=0$ and $P_x^2=P_y^2=[-a_1/(2b_1+b_2)]$, which coincides with a circularly polarized Sm*A*-type phase having the achiral symmetry C_{2v}. Hence, it is a biaxial phase with a transverse polar order. (ii) State V, obtained for $P_x=P_y=0$ and $\xi_x^2=\xi_y^2=[-\alpha_1/(2\beta_1+\beta_2)]$, which is associated with a Sm*C* achiral layer configuration of monoclinic symmetry C_{2h}. The absence of average transverse polarization in this configuration can be figured as resulting from an isotropic rotation of the molecules around the directors. Since we aim to analyze the coupling effects between tilt and polar orders, states IV and V will not be further discussed, except in Sec. III D.

III. MACROSCOPIC STRUCTURES OF THE MESOPHASES

A. Induced layer ordering

Let us first analyze the compatibility of the equilibrium molecular configurations found in Sec. II, with a layer order. The onset below the liquid phase of a layer ordering in the direction normal to $\hat{k}$ corresponds to the condensation of a scalar density wave associated with a two-component order parameter $\psi=|\psi|e^{i(\hat{k}\cdot\vec{r}+\alpha)}$ (and ψ^*), which transforms as a two-dimensional irreducible representation of the Euclidean symmetry group, denoted E_k in Ref. [10]. In our description, nonzero spontaneous values of ψ are induced by the "primary" tilt and polar-wave order parameters (ξ_i) and (η_i), and therefore result from the existence of coupling invariants which are linear in ψ. Using the transformation properties of the irreducible representations G_k and E_k (whose generating matrices are given in the Appendix), one finds that the lowest degree invariants correspond to $\psi=|\psi|e^{i(2kz+\alpha)}$, i.e., when the induced layer ordering possesses a wavelength with half the period of the transverse tilt and polar waves. Three independent invariants are found:

$$\begin{aligned}
I_5&=\xi_1\xi_2^*\psi^*+\xi_2\xi_1^*\psi\\
&=2|\psi|[\xi_x^2\cos(2\tilde{\varphi}_x-\alpha)+\xi_y^2\cos(2\tilde{\varphi}_y-\alpha)],\\
I_5'&=\eta_1\eta_2^*\psi^*+\eta_2\eta_1^*\psi\\
&=2|\psi|[P_x^2\cos(2\varphi_x-\alpha)+P_y^2\cos(2\varphi_y-\alpha)], \qquad (9)\\
I_6&=(-\eta_1\xi_2^*+\eta_2^*\xi_1)\psi^*+(\eta_2\xi_1^*-\eta_1^*\xi_2)\psi\\
&=4|\psi|[P_x\xi_x\cos(\varphi_x+\tilde{\varphi}_x-\alpha)+P_y\xi_y\cos(\varphi_y+\tilde{\varphi}_y-\alpha)].
\end{aligned}$$

The equilibrium values of $|\psi|$, arising below the liquid, are obtained by minimizing the following contribution to the Landau free-energy, with respect to $|\psi|$:

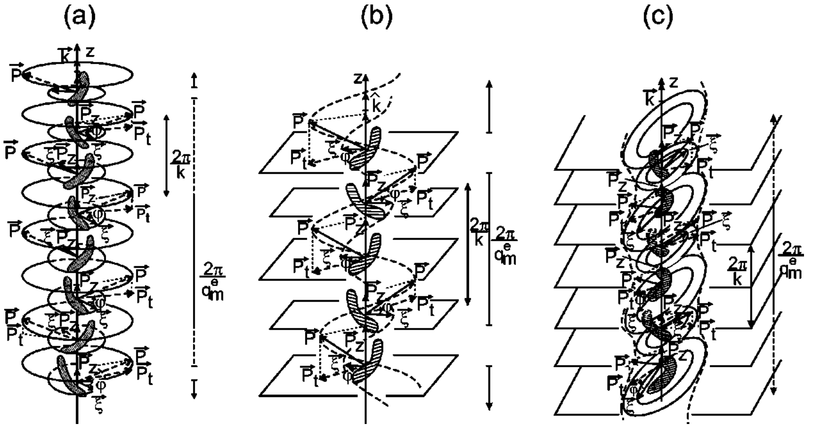

FIG. 4. Structure of the molecular configurations I′, II′, and III′. (a) Configuration I′ with circularly polarized transverse waves and biaxial cholesteric structure of chiral symmetry $P2_1$. (b) Bilayer smectic structure of the configuration II′ with linearly polarized transverse waves. The achiral symmetry is $Pmm2$ for the bilayer and m for the macroscopic structure. (c) Bilayer smectic structure of the configuration III′, with elliptically polarized transverse waves. The chiral symmetry is $P2$ for the bilayer and $P1$ for the macroscopic structure.

TABLE I. Equilibrium molecular configurations which may arise below an isotropic liquid formed from achiral molecules with transverse dipoles, as the result of a coupling between their tilt and transverse polar orders. The columns have the following meaning: (a) labeling of the mesophases; (b) equilibrium dephasing between the tilt and transverse polar waves, and corresponding relationship between the waves amplitudes; (c) equilibrium value of the longitudinal spontaneous polarization; and (d) type of polarization of the tilt and polar waves. States IV and V correspond to uncoupled waves.

(a)		(b)	(c)	(d)
I	$\tilde{\varphi}_x-\varphi_x=\tilde{\varphi}_y-\varphi_y=0,\pi$	$\xi_x=\xi_y, P_x=P_y$	$P_z^e=0$	circular
II		$\xi_x\neq 0, \xi_y=0, P_x\neq 0, P_y=0$		linear
III		$\xi_x^2\neq\xi_y^2, P_x^2\neq P_y^2$		elliptic
I′	$\tilde{\varphi}_x-\varphi_x=\tilde{\varphi}_y-\varphi_y\neq 0,\pi$	$\xi_x=\xi_y, P_x=P_y$	$P_z^e\neq 0$	circular
II′		$\xi_x\neq 0, \xi_y=0, P_x\neq 0, P_y=0$		linear
III′		$\xi_x^2\neq\xi_y^2, P_x^2\neq P_y^2$		elliptic
IV	$\tilde{\varphi}_x-\varphi_x=\tilde{\varphi}_y-\varphi_y=\pm\frac{\pi}{2}$	$\xi_x=\xi_y=0, P_x=P_y\neq 0$	$P_z^e=0$	circular
V		$\xi_x=\xi_y\neq 0, P_x=P_y=0,$		circular

$$F_e(|\psi|,\xi_x,\xi_y,P_x,P_y,\tilde{\varphi}_x,\tilde{\varphi}_y,\varphi_x,\varphi_y)=\frac{\gamma}{2}|\psi|^2+\nu_1 I_5+\nu_2 I_5'+\nu_3 I_6. \tag{10}$$

This gives

$$|\psi|^e=\left[-\frac{1}{\gamma}(\nu_1 I_5+\nu_2 I_5'+\nu_3 I_6)\right]^{1/2}. \tag{11}$$

Introducing successively in Eq. (11) the equilibrium values of the variational parameters for each of the stable configurations I–III and I′–III′, as given in Table I, yields the following conclusions. For the four configurations II, III, II′, and III′ one has $I_5\neq 0$, $I_5'\neq 0$, and $I_6\neq 0$, and therefore $|\psi|^e\neq 0$. *These configurations necessarily lead to the formation of a layer order*, whose periodicity is half the period of the tilt and polar waves. In contrast, for the configurations I and I′, one finds $I_5=I_5'=I_6=0$, i.e., *no layer order occurs for coupled transverse tilt and polar circular waves*.

B. Incommensurate modulations

In order to describe the long-range order for the mesophases having the local molecular configurations I–III and I′–III′, one needs to take into account the interactions between the molecules along the z direction, which is expressed phenomenologically by the inhomogeneous part F_i of the free-energy density. Using the transformation properties of the ξ_i and η_i components, and restricting ourselves to the inhomogeneous terms which are quadratic in those components, one finds three types of contributions to F_i:

(i) The Lifshits invariants, which express the dependence on z of the order-parameter components:

$$I_7=\left(\xi_1\frac{\partial\xi_1^*}{\partial z}-\xi_1^*\frac{\partial\xi_1}{\partial z}\right)+\left(\xi_2^*\frac{\partial\xi_2}{\partial z}-\xi_2\frac{\partial\xi_2^*}{\partial z}\right)\sim\xi_x^2\frac{\partial\tilde{\varphi}_x}{\partial z}+\xi_y^2\frac{\partial\tilde{\varphi}_y}{\partial z}, \tag{12}$$

$$I_7'=\left(\eta_1\frac{\partial\eta_1^*}{\partial z}-\eta_1^*\frac{\partial\eta_1}{\partial z}\right)+\left(\eta_2^*\frac{\partial\eta_2}{\partial z}-\eta_2\frac{\partial\eta_2^*}{\partial z}\right)\sim P_x^2\frac{\partial\varphi_x}{\partial z}+P_y^2\frac{\partial\varphi_y}{\partial z}.$$

(ii) The direct and inverse flexoelectric coupling invariants:

$$I_8=\left(\xi_1\frac{\partial\eta_1^*}{\partial z}-\xi_1^*\frac{\partial\eta_1}{\partial z}\right)+\left(\xi_2\frac{\partial\eta_2^*}{\partial z}-\xi_1^*\frac{\partial\eta_2}{\partial z}\right)\sim\xi_x\frac{\partial P_x}{\partial z}\sin\varphi_1+\xi_y\frac{\partial P_y}{\partial z}\sin\varphi_2+P_x\xi_x\frac{\partial\varphi_x}{\partial z}\cos\varphi_1+P_y\xi_y\frac{\partial\varphi_y}{\partial z}\cos\varphi_2, \tag{13}$$

$$I_8'=\left(\eta_1\frac{\partial\xi_1^*}{\partial z}-\eta_1^*\frac{\partial\xi_1}{\partial z}\right)+\left(\eta_2\frac{\partial\xi_2^*}{\partial z}-\eta_2^*\frac{\partial\xi_2}{\partial z}\right)\sim P_x\frac{\partial\xi_x}{\partial z}\sin\varphi_1+P_y\frac{\partial\xi_y}{\partial z}\sin\varphi_2-P_x\xi_x\frac{\partial\tilde{\varphi}_x}{\partial z}\cos\varphi_1-P_y\xi_y\frac{\partial\tilde{\varphi}_y}{\partial z}\cos\varphi_2.$$

(iii) The Ginzburg invariants which reflect the elastic energy:

$$I_9=\frac{\partial\xi_1}{\partial z}\frac{\partial\xi_1^*}{\partial z}+\frac{\partial\xi_2}{\partial z}\frac{\partial\xi_2^*}{\partial z}\sim\left(\frac{\partial\xi_x}{\partial z}\right)^2+\left(\frac{\partial\xi_y}{\partial z}\right)^2+\xi_x^2\left(\frac{\partial\tilde{\varphi}_x}{\partial z}\right)^2+\xi_y^2\left(\frac{\partial\tilde{\varphi}_y}{\partial z}\right)^2,$$

$$I_9' = \frac{\partial \eta_1}{\partial z}\frac{\partial \eta_1^*}{\partial z} + \frac{\partial \eta_2}{\partial z}\frac{\partial \eta_2^*}{\partial z} \sim \left(\frac{\partial P_x}{\partial z}\right)^2 + \left(\frac{\partial P_y}{\partial z}\right)^2 + P_x^2\left(\frac{\partial \varphi_x}{\partial z}\right)^2 + P_y^2\left(\frac{\partial \tilde{\varphi}_y}{\partial z}\right)^2, \tag{14}$$

$$\begin{aligned} I_{10} = & \left(\frac{\partial \eta_1}{\partial z}\frac{\partial \xi_1^*}{\partial z} + \frac{\partial \eta_1^*}{\partial z}\frac{\partial \xi_1}{\partial z}\right) - \left(\frac{\partial \eta_2}{\partial z}\frac{\partial \xi_2^*}{\partial z} + \frac{\partial \eta_2^*}{\partial z}\frac{\partial \xi_2}{\partial z}\right) \\ & \sim \left(\frac{\partial P_x}{\partial z}\frac{\partial \xi_x}{\partial z} + P_x \xi_x \frac{\partial \varphi_x}{\partial z}\frac{\partial \tilde{\varphi}_x}{\partial z}\right)\cos\varphi_1 \\ & + \left(\frac{\partial P_y}{\partial z}\frac{\partial \xi_y}{\partial z} + P_y \xi_y \frac{\partial \varphi_y}{\partial z}\frac{\partial \tilde{\varphi}_y}{\partial z}\right)\cos\varphi_2 \\ & + \left(P_x \frac{\partial \xi_x}{\partial z}\frac{\partial \varphi_x}{\partial z} - \xi_x \frac{\partial P_x}{\partial z}\frac{\partial \tilde{\varphi}_x}{\partial z}\right)\sin\varphi_1 \\ & + \left(P_y \frac{\partial \xi_y}{\partial z}\frac{\partial \varphi_y}{\partial z} - \xi_y \frac{\partial P_y}{\partial z}\frac{\partial \varphi_y}{\partial z}\right)\sin\varphi_2. \end{aligned}$$

Therefore the inhomogeneous free energy density has the form

$$F_i(\xi_x, \xi_y, P_x, P_y, \tilde{\varphi}_x, \tilde{\varphi}_y, \varphi_x, \varphi_y) = \mu_1 I_7 + \mu_1' I_7' + \mu_2 I_8 + \mu_2' I_8' + K_1 I_9 + K_1' I_9' + K_2 I_{10}, \tag{15}$$

where μ_1, μ_1', μ_2, μ_2', K_1, K_1', and K_2 are phenomenological coefficients. One can pose

$$\frac{\partial \tilde{\varphi}_x}{\partial z} = \frac{\partial \tilde{\varphi}_y}{\partial z} = \frac{\partial \varphi_x}{\partial z} = \frac{\partial \varphi_y}{\partial z} = q, \tag{16}$$

where q is a modulation wave vector, and assume for the three configurations that ξ_x, ξ_y, P_x, and P_y are slowly varying periodic functions of z, with the periodicity $(2\pi/q)(q \ll k)$. Taking

$$\xi_x = \xi_o \cos qz, \quad \xi_y = \xi_o \sin qz,$$

$$P_x = P_o \cos qz, \quad P_y = P_o \sin qz \tag{17}$$

one can then express the homogeneous and inhomogeneous parts of the free-energy density as

$$\begin{aligned} F_h = & \frac{\alpha_1}{2}\ \xi_o^2 + \frac{\xi_o^4}{2}\left(\beta_1 + \frac{\beta_2}{2}\cos^2 qz \sin^2 qz\right) + \frac{a_1}{2}\ P_o^2 \\ & + \frac{P_o^4}{2}\left(b_1 + \frac{b_1}{2}\cos^2 qz \sin^2 qz\right) \\ & + \delta_1 \xi_o P_o[\cos^2 qz \cos\varphi_1 + \sin^2 qz \cos\varphi_2] + \frac{\delta_2}{2}\xi_o^2 P_o^2 \\ & + \frac{\delta_3}{2}\xi_o^2 P_o^2[\cos^2 qz \cos\varphi_1 + \sin^2 qz \cos\varphi_2]^2 \\ & + \mu P_z \xi_o P_o[\cos^2 qz \sin\varphi_1 + \sin^2 qz \sin\varphi_2] + \frac{1}{2\chi_{33}^o}P_z^2, \end{aligned} \tag{18}$$

$$\begin{aligned} F_i = & q^2[2(K_1\xi_o^2 + K_1' P_o^2) + K_2 \xi_o P_o(\cos\varphi_1 + \cos\varphi_2)] \\ & + q\{(\mu_1 \xi_o^2 + \mu_1' P_o^2) + \xi_o P_o[(\mu_2 + \mu_2') \\ & \times \sin qz \cos qz(\sin\varphi_2 - \sin\varphi_1) + (\mu_2 - \mu_2') \\ & \times(\cos^2 qz \cos\varphi_1 + \sin^2 qz \cos\varphi_2]\}, \end{aligned} \tag{19}$$

minimization of the total free-energy $\Phi = \int(F_h + F_i)dz$ with respect to q yields the equilibrium values

$$q^e = -\frac{1}{4}\frac{[\mu_1\xi_o^2 + \mu_1' P_o^2 + (\mu_2 - \mu_2')P_o\xi_o]}{[K_1\xi_o^2 + K_1' P_o^2 + K_2 P_o \xi_o]} \tag{20}$$

for phases I, II, and III. Using the approximations

$$\xi_o \simeq \left[\frac{\alpha_o(T_c - T)}{2\beta_1 + \beta_2}\right]^{1/2}$$

and

$$P_o \simeq \left[\frac{a_o(T_c - T)}{2b_1 + b_2}\right]^{1/2}$$

shows that in those phases there is a *constant* long-period modulation, of periodicity $2\pi/q^e$, which is incommensurate with the wave period $2\pi/k$. For phases I′, II′, and III′, one finds

$$q'^e = -\frac{1}{4}\frac{(\mu_1\xi_o^2 + \mu_1' P_o^2)}{[K_1\xi_o^2 + K_1' P_o^2 + K_2 P_o\xi_o \cos\varphi_1]}, \tag{21}$$

which depends on temperature via the angle φ_1. Therefore, the long-period modulation is temperature dependent. Note that the preceding results were obtained using first approximations, and the lowest-degree inhomogeneous terms. Taking into account higher-degree gradient invariants or less stringent approximations would lead to more complex behaviors.

C. Structure and nature of the mesophases

We are now able to describe the structure of the mesophases corresponding to the six equilibrium molecular configurations disclosed in Sec. II. Denoting the mesophases as the corresponding configurations, the structures can be depicted as follows:

(a) Mesophases I and I′. In mesophase I the director $\hat{n}$ and transverse polarization $\vec{P}_t$ describe two concentric spirals around the z axis with a circular basis, as shown in Fig. 2(a). Since there is no layer order the mesophase has a *biaxial cholesteric structure* with a chiral symmetry D_∞. Along the z direction one has the superimposition of two incommensurate modulations with constant periodicities $2\pi/k$ and $2\pi/q_I^e$ [where q_I^e is given by Eq. (20)]. This destroys the strict antiferroelectric character of the structure that would exist in the absence of the incommensurate modulation, and in particular the discrete helical rotations $\{\vec{t}_{\varphi/k}\}$, where c_φ is a rotation around z of angle φ, and $\vec{t}_{\varphi/k}$ a discrete translation along z. Note that biaxial cholesteric phases have been already found experimentally in lyotropic systems [11,12].

At variance with mesophase I, mesophase I′ possesses a longitudinal component P_z for the total polarization $\vec{P}$. $\vec{P}$ is located within the tilt plane $(\hat{n},\hat{k})$ at an angle $(\pi/2)-\theta$ with $\hat{k}$, and therefore fulfills the $\hat{n}\rightarrow-\hat{n}$ symmetry but not the up-down $(\hat{k}\rightarrow-\hat{k})$ symmetry of the layers. Hence the mesophase has a biaxial cholesteric structure of chiral polar symmetry $P2_1$, represented in Fig. 4(a), and formed by two concentric spirals associated with the vectors $\vec{\xi}$ and $\vec{P}$. Note that the structure may split into mesoscopic domains of opposed polarities $\pm P_z$ corresponding to opposed-phase configurations for $\vec{\xi}$ and $\vec{P}_t$. Due to the influence of the modulation wave of period $2\pi/q'e$, which varies with the temperature *T*, the periodicity along *z* is destroyed and an overall chiral polar symmetry C_∞ is restored for the macroscopic structure, with an incommensurate layer periodicity.

(b) Mesophases II and II′. Mesophase II corresponds to an *antiferroelectric bilayer structure*, as shown in Fig. 2(b), with opposed tilt and transverse polarizations in two successive layers. It coincides in average with a SmC_A^* type structure found in sticklike antiferroelectric systems [13]. However, since the molecular orientation distribution function follows a sinusoidal wave along *z*, the structure should differ from that of a standard SmC_A^* mesophase by large fluctuations of the tilt and polarization around their average orientations. One has an *achiral* orthorhombic symmetry mma for the bilayers, each layer being a glide plane (a). The incommensurate modulation q^e given by Eq. (20), which varies with *T*, destroys the strict bilayer periodicity, and, since the orientation of the tilt and polarization vectors $\vec{\xi}$ and $\vec{P}_t$ is arbitrary in the (x,y) plane, it gives rise to a long-period spiral, i.e., $\vec{\xi}$ and $\vec{P}_t$ rotate slightly from one layer to another.

Similar considerations apply to mesophase II′, which differs from mesophase II by the orientation of the polarization $\vec{P}$. The existence of a longitudinal component P_z makes the structure to be ferroelectrically ordered along *z*. As a result the transverse twofold rotations are lost and the symmetry of a bilayer is lowered to $Pmm2_1$, violating the $\hat{k}\rightarrow-\hat{k}$ symmetry. An analogous bilayer structure was predicted theoretically for sticklike molecules in Ref. [14]. The modulation wave-vector q'^eyields again a long pitch spiral rotation of the molecules which destroys the strict bilayer periodicity [Fig. 4(b)].

(c) Mesophases III and III′. Mesophase III has a basic ferrielectric bilayer smectic structure, with transverse polarization $\vec{P}_t$. Each bilayer has the orthorhombic 2_1 22 chiral symmetry, being formed by two concentric spirals of elliptic basis with vectors $\vec{\xi}$ and $\vec{P}_t$ of opposed polarities and different lengths for two successive layers. Along the spirals the $\vec{\xi}$ and $\vec{P}_t$ moduli vary, as shown in Fig. 2(c). Along *z* the bilayer order is incommensurately modulated with a constant modulation wave vector q^e, given by Eq. (19), which destroys the helical rotation 2_1 and leads to the macroscopic twofold polar symmetry 2. Mesophase III′ differs from mesophase III by the onset of a longitudinal component of the polarization P_z^e, and a long wave modulation $q'e$ varying with *T*. The symmetry of a bilayer is lowered to $P2_1$, and the macroscopic symmetry becomes triclinic 1 [Fig. 4(c)].

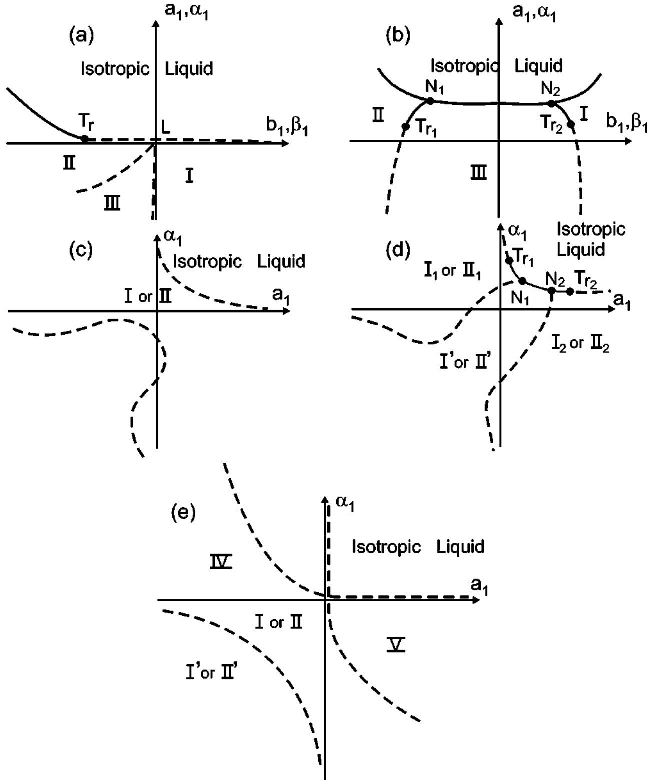

FIG. 5. Theoretical phase diagrams obtained by the minimization of the thermodynamic potential Φ. Solid and dashed lines are first- and second-order transition lines, respectively. *L* is a Landau point. T_r and *N* designate tricritical and three-phase points, respectively. I_1 and I_2 (or II_1 and II_2) are isostructural phases.

D. Phase diagrams

The relevant theoretical phase diagrams associated with the molecular systems under consideration are two dimensional, since one can in general vary not more than two external variables, e.g., the temperature *T* and the relative concentration in a mixture of two types of molecular subunits. As the regions of stability of the full set of stable states (I–III and I′–III′) can be obtained only by varying at least three phenomenological coefficients, as for example a_1, α_1, and δ (or b_1 or β_1), we will consider two-dimensional cuts of the corresponding three-dimensional phase diagrams, i.e., in the planes (a_1,α_1) and (a_1,b_1) or (α_1,β_1). Minimization of the full thermodynamic potential $\Phi=\int(F_h+F_i)dz$ with respect to the variational parameters yields the four phase diagrams which are shown in Figs. 5(a)–5(d).

Figure 5(a) shows the respective regions of stability of mesophases I, II, and III in the (a_1,b_1) or (α_1,β_1) phase diagrams, in the case of an eighth-degree expansion of F_h, which is the minimal degree necessary to obtain a stable mesophase III. This mesophase is separated from mesophases I and II by second-order transition lines, and merge with the isotropic liquid phase at a four-phase ‘‘Landau’’ point. In order to have a direct transition to mesophase III from the isotropic liquid, one needs to expand F_h at least up to the tenth degree. The corresponding phase diagram shown in Fig. 5(b) reveals that the transitions to the mesophases I, II, and III are, in this case, always first-order [15].

The regions of stability of mesophases I′ and II′ are obtained in the plane (a_1,α_1), and represented in Figs. 5(c) and 5(d). The phase diagram of Fig. 5(c) corresponds to a fourth-degree expansion of F_h, and is obtained either for mesophases I and I′ or for mesophases II and II′. One can verify that the primed mesophases can be reached from the isotropic liquid only across the regions of stability of mesophases I or II, i.e., across two second-order transitions. The phase diagram of Fig. 5(d) requires a least a sixth-degree expansion for F_h. Here phases I′ and II′ can be reached from the isotropic liquid across a first-order transition line. Note that the primed phases separate two distinct regions of stability of the unprimed phases corresponding to isostructural phases. A direct first-order transition from the liquid to mesophase III′ would require an eighth-degree expansion of F_h. Finally, Fig. 5(e) shows the location in the (α_1, a_1) plane of phases IV and V, which result from uncoupled tilt and polar waves, with respect to the phases I (or I′) and II (or II′).

IV. FIELD EFFECTS

In this section we analyze the physical effects produced by application of an electric field $\vec{E}$ to the different mesophases found in Sec. III. We shall separately examine the effects induced by the application of a longitudinal field E_z and of a transverse field $\vec{E}_t = E_x\vec{e}_x + E_y\vec{e}_y$.

A. Longitudinal field effects

When applying an electric field along the *z* direction, the homogeneous free-energy density becomes $F_h^{E_z} = F_h - E_z P_z$, where F_h is given by Eq. (5). Minimizing $F_h^{E_z}$ with respect to P_z gives the equilibrium expression

$$P_z^e(E_z) = \chi_{33}^o E_z - \mu\, \chi_{33}^o (P_x \xi_x \sin\varphi_1 + P_y \xi_y \sin\varphi_2), \tag{22}$$

which is the sum of induced and spontaneous contributions. Introducing $P_z^e(E_z)$ in $F_h^{E_z}$ and minimizing again $F_h^{E_z}$ with respect to the dephasings φ_1 and φ_2, yields the equations of state

$$\begin{aligned} P_x \xi_x \sin\varphi_1 \left(\delta_1 + \delta_3 \frac{I_3}{4} \right) &+ \mu \chi_{33}^o \cos\varphi_1 \\ &\times [E_z - \mu (P_x \xi_x \sin\varphi_1 + P_y \xi_y \sin\varphi_2)] = 0, \end{aligned} \tag{23}$$

$$\begin{aligned} P_y \xi_y \sin\varphi_2 \left(\delta_1 + \delta_3 \frac{I_3}{4} \right) &+ \mu \chi_{33}^o \cos\varphi_2 \\ &\times [E_z - \mu (P_x \xi_x \sin\varphi_1 + P_y \xi_y \sin\varphi_2)] = 0. \end{aligned}$$

These equations reveal that mesophases I, II, and III, which correspond to $\sin\varphi_i = 0$ and $\cos\varphi_i = \pm 1 (i=1,2)$, *become unstable under the application of a longitudinal field*. Therefore applying such field to mesophases I, II, and III switches the system to the stable mesophases I′, II′, and III′, respectively. In the ‘‘primed’’ mesophases, application of a longitudinal field preserves the equilibrium relationships $\sin\varphi_1^e = \sin\varphi_2^e$ (for mesophases I′ and III′) or $\sin\varphi_1^e \neq 0$ (for mesophase II′), the values of φ_1^e and φ_2^e becoming temperature *and* field dependent. The unprimed → primed mesophase switching under application of finite E_z corresponds to a discontinuous rotation, of angle $\varphi_1^e = \varphi_2^e \neq (0,\pi)$, with respect to its initial position $[\varphi_1^e = \varphi_2^e = (0,\pi)]$ of the transverse component $\vec{P}_t$ of the total polarization $\vec{P}$. Note that above a threshold field E_z^e, corresponding to the unwinding of the helixes in phases I′, II′, and III′, the total polarization $\vec{P}$ is oriented along *z*, and the molecular director is located in average in a direction normal to z. Such configuration coincides with a biaxial Sm*A* type of phase, with the smectic planes oriented orthogonally to the (x,y) plane.

B. Transverse field effects

The transverse field $\vec{E}_t = (E_x, E_y)$ transforms as the irreducible representation denoted E_1 in Ref. [10], whose generating matrices are given in the Appendix. Using the symmetry properties of $G_{\hat{k}}$ and E_1 allows the construction of two coupling invariants between the order-parameter components and $\vec{E}_t$, which are

$$I_{11} = (E_x^2 + E_y^2)(\eta_1 \eta_2 + \eta_1^* \eta_2^*) \sim E_t^2 (P_x^2 - P_y^2), \tag{24}$$

$$I_{12} = E_x E_y (\eta_1 \eta_1^* + \eta_2 \eta_2^*) \sim E_x E_y (P_x^2 + P_y^2). \tag{25}$$

Note that the preceding biquadratic forms express nonlinear piezoelectric effects, due to the coupling of the transverse tilt and polar waves, which result from the different symmetries of E_t and P_t.

Minimizing the homogeneous free-energy density $F_h^{E_t} = F_h - I_{11} - I_{12}$ with respect to P_x and P_y yields the equation of state

$$\begin{aligned} (P_x - P_y)[a_1 &+ b_1(P_x^2 + P_y^2) - b_2 P_x P_y \sin^2(\varphi_x - \varphi_y) \\ &+ \delta_2(\xi_x^2 + \xi_y^2) - \delta_3 \xi_x \xi_y \cos\varphi_1 \cos\varphi_2 \\ &+ \mu^2 \chi_{33}^o \xi_x \xi_y \sin\varphi_1 \sin\varphi_2 - 2E_x E_y] \\ &+ \delta_1(\xi_x \cos\varphi_1 - \xi_y \cos\varphi_1) + \delta_3(P_x \xi_x^2 \cos^2\varphi_1 \\ &- P_y \xi_y^2 \cos^2\varphi_2) - \mu^2 \xi_{33}^o (P_x \xi_x^2 \sin^2\varphi_1 - P_y \xi_y^2 \sin^2\varphi_2) \\ &+ 2E_t^2 (P_x + P_y) = 0, \end{aligned} \tag{26}$$

showing that mesophases I and I′ (corresponding to the equilibrium relationship $P_x = P_y, \xi_x = \xi_y, \varphi_1 = \varphi_2$) *become unstable under the application of a transverse field*. Therefore, applying a transverse field switches phases I and I′ to phases III and III′ $(P_x \neq P_y, \xi_x \neq \xi_y)$, respectively. In other words the circularly polarized molecular configurations of the layers will be elliptically distorted, with the long axes of the ellipses along the direction of the applied field. The switching from phase I to phase III or from phase I′ to phase III′ will give rise to a remarkable *field induced stratification of a cholesteric structure* which to our knowledge has not been reported previously in liquid crystal systems. The stratification process may occur continuously when increasing E_t continuously from zero. On the other hand, applying a transverse field to mesophases II and II′ will have the effect of orienting the direction of the linearly polarized wave along the field, i.e., to turn the molecular director and polarization around the *z* direction.

V. SUMMARY AND DISCUSSION

In this paper a phenomenological description has been made of the mesophases which may arise below a liquid formed from achiral molecules having a transverse dipole, as the result of a coupling between their tilt and polar orders. Our results can be summarized as follows

(1) Six stable mesophases have been found, which have been denoted I–III and I′–III′. Mesophases I–III correspond to tilt and polar waves which are in phase or in phase opposition, and were predicted theoretically in Ref. [9]. Mesophase I has a cholesteric biaxial structure with circularly polarized tilt and polar waves. Mesophases II and III are bilayer antiferroelectric and ferroelectric smectic structures, respectively associated with linearly and elliptically polarized waves. Mesophases I′, II′, and III′ differ from their unprimed analogs by an arbitrary dephasing between the tilt and polar waves, which gives rise to a spontaneous out-of-plane polarization, having a nonzero longitudinal component P_z^e.

(2) Phase diagrams involving the six mesophases show that mesophases I′–III′ can be reached from the liquid state either across the regions of stability of mesophases I–III, via two second-order transitions, or directly across a first-order transition.

(3) Assuming slowly varying sinusoidal dependences of the wave amplitudes ξ_x, ξ_y, P_x, and P_y, as functions of the *z* coordinate, the structures of the six mesophases are found to be incommensurately modulated. The modulation wave vectors can be either constant (for mesophases I–III), or vary with temperature (for mesophases I′–III′).

(4) Under application of a longitudinal electric field, mesophases I–III become unstable, and the tilt and spontaneous polarizations are switched to their configurations in the mesophases I′–III′, respectively. When applying a transverse electric field, the cholesteric structures of the mesophases I and I′ are elliptically deformed, and transform into the smectic structures of the mesophase III and III′. A transverse field also results in a reorientation of the linearly polarized waves, in mesophases II and II′.

The preceding results are valid not only for bent shaped molecules of symmetry $C_{2v}(mm2)$, but for any achiral molecular configuration displaying a transverse polar order. Figure 6 shows the other possible achiral molecular configurations having a transverse polar order. They possess the polar symmetries $C_s(m)$, $C_{nv}(n=2,3,4,5,\ldots)$, and $C_{\infty v}$. Note also that only tilted mesophases have been considered in our study. Nontilted mesophases which may arise below the liquid states, such as the biaxial Sm*A* type phase predicted theoretically in Ref. [8], are associated with different equilibrium values of the order-parameter components.

Mesophases I′, II′, and III′ result from the coupling of the tilt and polar waves, and are stabilized when the vector product $\vec{\xi}\times\vec{P}_t$ is nonzero, i.e., when the angle between the two vector waves is different than $(0,\pi)$. Hence the longitudinal polarization component $P_z \simeq \vec{\xi}\times\vec{P}_t$ is due to *a nonlinear piezoelectric effect* arising from the conjuncted existence of dephased tilt and transverse polar waves. Such an effect was already pointed out in chiral antiferroelectric [14] and ferroelectric [16] liquid crystal systems.

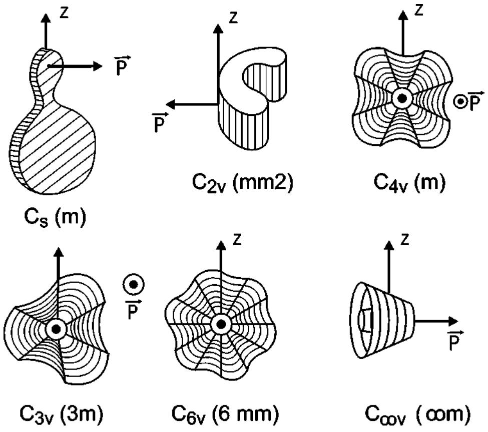

FIG. 6. Illustration of the molecular symmetries $C_s, C_{nv}(n=2,3,4,6)$ and $C_{\infty v}$, with transverse polar order.

The biaxial cholesteric nature of mesophase I was overlooked in Ref. [9], as well as the incommensurate modulation of the structure of this mesophase, which destroys the periodicity of the tilt and polar waves $(2\pi/k)$. On the other hand, the authors of Ref. [9] stressed the analogy of their model, based on a single transverse polar wave, with the two-dimensional isotropic *d*-pairing wave model of superconductivity discussed by Gufan *et al.* [17]. One can note that there is also a one-to-one correspondence between the anisotropic *d*-pairing wave model examined in Ref. [17] and the approach proposed by Roy *et al.* [8] for describing the liquid crystal phases formed from bent shaped molecules, below a Sm*A* phase. In this respect one can show [18] that the phenomenological approach developed in the present paper is equivalent in layered superconductors to an extended *d*-wave pairing model $(d+d')$ in which two dephased *d*-pairing wave functions are the analogs of the tilt and polar transverse waves. The physical analogs of the spontaneous polarization component P_z and associated second-order piezoelectric effect are, respectively, a spontaneous polarization normal to the superconducting layers and a second-order magnetoelectric effect [18], previously discussed in Ref. [19].

Let us briefly compare the experimental results which have been reported for the structures of the mesophases formed from bent shaped molecules (labeled *B*1–*B*7 following a recent proposed nomenclature [20]) with our theoretical results. Although there exists, at present, only a partial understanding of those structures [5], the following observations can be made.

(1) A possible candidate for realizing the biaxial cholesteric structures (mesophases I and I′) predicted in our approach is the so-called *B*7 phase [5,21], which is found in nitrosubstituted compounds, and obtained by fast cooling from the liquid. No layer order was reported for this phase, which shows unusual textures (which are not comparable with the textures of the other *B* mesophases) with circular domains growing like a spiral. Such domains are reminiscent of a cholesteric structure [22]. The helicoidal structure of the *B*7 phase contains an equal number of right-and-left-handed

helicoidal domains [5] that would coincide with the in-phase and opposed-phase configurations predicted for mesophase I.

(2) In the structure of the $B6$ phase, which is a tilted smectic phase without in-plane order, the layer spacing has been found to be smaller that the half length of the molecules [5]. This property coincides with the prediction of the interlayer distance found for the smectic structures of mesophases II, III and II$'$, III$'$, which is half the period of the transverse waves, corresponding to a full rotation of the molecules around the z axis.

(3) The $B2$ mesophase, which has been the most investigated of the B mesophases [and has been designated as SmAb(7), SmCP_A(4), SmX_1 [23], and $M1$ [24]], possesses a number of features which also characterize mesophases II$'$ and II$'$ in our study. Thus, it is a biaxial tilted smectic phase having a bilayer antiferroelectric order [3–5,25] with a typical antiferroelectric switching behavior, the switched state being found to be independent of the polarity of the electric field [26]. Regions where the texture of the switched state is different for the opposite sign of the applied electric field were also reported [4], that may correspond to the mesoscopic domains of opposed polarization into which mesophase II$'$ may split. Sekine *et al.* [7] also suggested a helicoidal structure, with helixes of both handedness, that would correspond to coexisting in-phase and opposed-phase configurations for the mesophase II$'$.

Mesophase $B1$, which appears below the isotropic phase, and $B5$, which is obtained on cooling the $B2$ phase, seem to possess a two-dimensional in-plane order [5], and therefore are out of the framework of the present study. This is also the case for the $B3$ and $B4$ phases, which are assumed to display a crystalline type of order [5].

ACKNOWLEDGMENTS

The authors are grateful to C. E. I. Carneiro for helpful discussions, and to Fundação de Amparo à Pesquisa do Estado de São Paulo for financial support.

APPENDIX

In this appendix we give the generating matrices associated with the irreducible representation $G_{\hat{k}}$, E_k, and E_1, labeled as in Ref. [10], which allow one to construct the basic and coupling invariants used in our approach. The symmetry operations C_φ, $\sigma_{v\varphi}$, and I denote, respectively, a rotation of angle φ around the z axis, a vertical plane turned by an angle φ with respect to x axis, and the inversion.

$$
\begin{array}{cccc}
 & \{C_\varphi|kz\} & \{\sigma_{v\varphi}|kz\} & \{I|0\} \\
G_{\hat{k}} &
\begin{bmatrix} e^{i\varphi}e^{ikz} & & & 0 \\ & e^{-i\varphi}e^{-ikz} & & \\ & & e^{i\varphi}e^{-ikz} & \\ 0 & & & e^{-i\varphi}e^{ikz} \end{bmatrix} &
\begin{bmatrix} & e^{2i\varphi}e^{-ikz} & & 0 \\ e^{-2i\varphi}e^{ikz} & & & \\ & & & e^{2i\varphi}e^{ikz} \\ & 0 & e^{-2i\varphi}e^{-ikz} & \end{bmatrix} &
\begin{bmatrix} & 0 & 1 & \\ & & & 1 \\ 1 & & 0 & \\ & 1 & & \end{bmatrix} \\
E_k &
\begin{bmatrix} e^{ikz} & \\ & e^{-ikz} \end{bmatrix} &
\begin{bmatrix} e^{ikz} & \\ & e^{-ikz} \end{bmatrix} &
\begin{bmatrix} & 1 \\ 1 & \end{bmatrix} \\
E_1 &
\begin{bmatrix} e^{i\varphi} & \\ & e^{-i\varphi} \end{bmatrix} &
\begin{bmatrix} & e^{2i\varphi} \\ e^{-2i\varphi} & \end{bmatrix} &
\begin{bmatrix} -1 & \\ & -1 \end{bmatrix}
\end{array}
$$

[1] F. Tournilhac, L. M. Blinov, J. Simon, and S. V. Yablonsky, Nature (London) **359**, 621 (1992).

[2] L. M. Blinov, Liq. Cryst. **24**, 143 (1998), and references therein.

[3] T. Niori, T. Sekine, J. Watanabe, T. Furukawa, and H. Takezoe, J. Mater. Chem. **6**, 1231 (1996).

[4] D. R. Link, G. Natale, R. Shao, J. E. Maclennan, N. A. Clark, E. Körblova, and D. M. Walba, Science **278**, 1924 (1997).

[5] G. Pelzl, S. Diele, and W. Weissflog, Adv. Mater. **11**, 707 (1999).

[6] S.-W. Choi, M. Zennyoji, Y. Takanishi, H. Takezoe, T. Niori, and J. Watanabe, Mol. Cryst. Liq. Cryst. **238**, 177 (1999).

[7] T. Sekine, T. Niori, M. Sone, J. Watanabe, S.-W. Choi, Y. Takanishi, and H. Takezoe, Jpn. J. Appl. Phys. **36**, 6455 (1997).

[8] A. Roy, N. V. Madhusudana, P. Tolédano, and A. M. Figueiredo Neto, Phys. Rev. Lett. **82**, 1466 (1999).

[9] V. L. Lorman and B. Mettout, Phys. Rev. Lett. **82**, 940 (1999).

[10] J. C. Tolédano and P. Tolédano, *The Landau Theory of Phase Transitions* (World Scientific, Singapore, 1987), Chap. 7.

[11] A. M. Figueiredo Neto, Y. Galerne, and L. Liébert, J. Phys. Chem. **89**, 3939 (1985).

[12] G. Melnik and A. Saupe, Mol. Cryst. Liq. Cryst. **145**, 95 (1987).

[13] V. L. Lorman, A. A. Bulbitch, and P. Tolédano, Phys. Rev. E **49**, 1367 (1994).

[14] P. Tolédano, A. M. Figueiredo Neto, A. A. Boulbitch, and A. Roy, Phys. Rev. E **59**, 6785 (1999).

[15] P. Tolédano and V. Dmitriev, *Reconstructive Phase Transitions* (World Scientific, Singapore, 1996), Chap. 1.

[16] P. Tolédano and A. M. Figueiredo Neto, Phys. Rev. Lett. **79**, 4405 (1997).

[17] Yu. M. Gufan, G. M. Vereshkov, P. Tolédano, B. Mettout, R. Bouzerar, and V. Lorman, Phys. Rev. B **51**, 9219 (1995).

[18] P. Tolédano and A. M. Figueiredo Neto, Phys. Rev. Lett. **84**, 5540 (2000).

[19] B. Mettout, P. Tolédano, and V. Lorman, Phys. Rev. Lett. **77**, 2284 (1996).

[20] Report of the Workshop ‘‘Chirality by Achiral Molecules’’ (Berlin, 1997) [Liq. Cryst. Today **9**, 1 (1999)].

[21] G. Pelzl, S. Diele, A. Jákli, C. Lischka, I. Wirth, and W. Weissflog, Liq. Cryst. **26**, 135 (1999).

[22] L. Bourdon, I. Sommeria, and M. Kleman, J. Phys. (France) **43**, 77 (1982).

[23] T. Niori, T. Sekine, J. Watanabe, T. Furukawa, and H. Takezoe, Mol. Cryst. Liq. Cryst. **301**, 337 (1997).

[24] S. Diele, S. Grande, H. Kruth, C. Lischka, G. Pelzl, W. Weissflog, and I. Wirth, Ferroelectrics **212**, 169 (1998).

[25] G. Pelzl, S. Diele, S. Grande, A. Jákli, C. Lischka, H. Kresse, H. Schmalfuss, I. Wirth, and W. Weissflog, Liq. Cryst. **26**, 401 (1999).

[26] A. Jákli, S. Rauch, D. Lötzsch, and G. Heppke, Phys. Rev. E **57**, 6737 (1998).